Intracortical Remodeling Parameters are Associated with Measures of Bone Robustness

HAVIVA M. GOLDMAN,[1,2]* NAOMI A. HAMPSON,[2] J. JARED GUTH,[1] DAVID LIN,[1] AND KARL J. JEPSEN[3]

[1]Department of Neurobiology and Anatomy, Drexel University College of Medicine, Philadelphia, Pennsylvania

[2]Department of Materials Science and Engineering, Drexel University College of Engineering, Philadelphia, Pennsylvania

[3]Department of Orthopaedic Surgery, University of Michigan, Ann Arbor, Michigan

ABSTRACT

Prior work identified a novel association between bone robustness and porosity, which may be part of a broader interaction whereby the skeletal system compensates for the natural variation in robustness (bone width relative to length) by modulating tissue-level mechanical properties to increase stiffness of slender bones and to reduce mass of robust bones. To further understand this association, we tested the hypothesis that the relationship between robustness and porosity is mediated through intracortical, BMU-based (basic multicellular unit) remodeling. We quantified cortical porosity, mineralization, and histomorphometry at two sites (38% and 66% of the length) in human cadaveric tibiae. We found significant correlations between robustness and several histomorphometric variables (e.g., % secondary tissue [$R^2 = 0.68$, $P < 0.004$], total osteon area [$R^2 = 0.42$, $P < 0.04$]) at the 66% site. Although these associations were weaker at the 38% site, significant correlations between histological variables were identified between the two sites indicating that both respond to the same global effects and demonstrate a similar character at the whole bone level. Thus, robust bones tended to have larger and more numerous osteons with less infilling, resulting in bigger pores and more secondary bone area. These results suggest that local regulation of BMU-based remodeling may be further modulated by a global signal associated with robustness, such that remodeling is suppressed in slender bones but not in robust bones. Elucidating this mechanism further is crucial for better understanding the complex adaptive nature of the skeleton, and how interindividual variation in remodeling differentially impacts skeletal aging and an individuals' potential response to prophylactic treatments. Anat Rec, 297:1817–1828, 2014.

Key words: complex adaptive system; robustness; remodeling; cortical bone; porosity

Grant sponsor: US Department of Defense; Grant numbers: (DoD) W81XWH-09-2-0113 and W81XWH-07-C-0097; Grant sponsor: NIH; Grant number: AR44927.

*Correspondence to: Haviva M. Goldman, PhD, Department of Neurobiology and Anatomy, Drexel University College of Medicine, 2900 Queen Lane, Philadelphia, PA 19129. Fax: 2158439082. E-mail: hgoldman@drexelmed.edu

Received 5 February 2014; Accepted 21 May 2014.

DOI 10.1002/ar.22962

Published online 25 June 2014 in Wiley Online Library (wileyonlinelibrary.com).

Previous research has demonstrated that a relationship exists between external bone size and tissue level mechanical properties (Currey, 1979; Tommasini et al., 2005; Jepsen et al., 2011; Epelboym et al., 2012). Further, variation in tissue modulus among individuals was shown to arise through modulation of both mineralization and porosity (Jepsen et al., 2011). Specifically, slender tibiae (narrow relative to length) had a lower porosity and higher ash content than more robust tibiae (wide relative to length). Modulating both mineralization and porosity has the advantage of expanding the range in which tissue modulus varies among individuals and minimizing mass in robust bones (Currey and Alexander, 1985). However, if this modulation reflects a suppression of intracortical remodeling [i.e., BMU or basic multicellular unit based remodeling, reflecting a defined area of bone formation followed by bone resorption (Frost, 1969)], this could lead to unrepaired microdamage in slender boned individuals and an increased skeletal fragility. Further, as intracortical remodeling is a central biological process that occurs throughout growth and with aging, lifelong suppression of remodeling would have significant effects on bone properties, fracture risk, and possibly the response to anticatabolic treatment regimens. Thus, understanding how BMU-based remodeling is regulated is clinically important. The goal of this study was to determine whether the relationship between robustness and porosity (Jepsen et al., 2011) was mediated through intracortical, BMU-based remodeling.

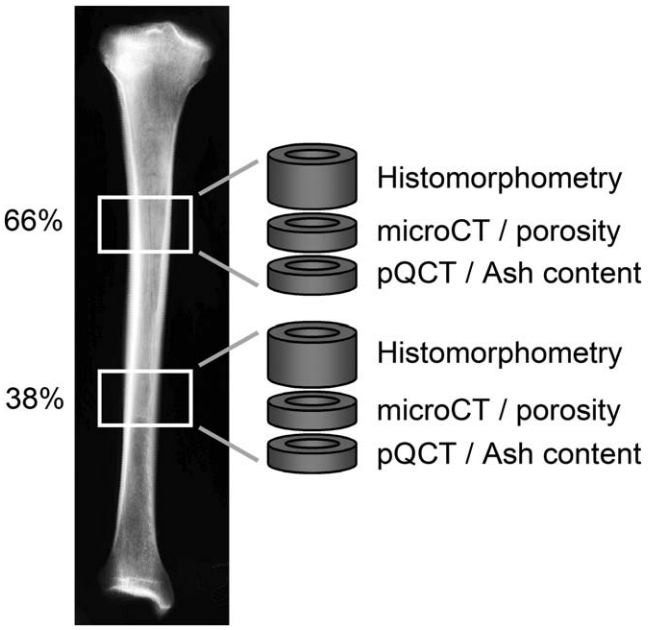

Fig. 1. Schematic showing how tibiae were processed to acquire porosity, composition, and histomorphometric measurements at the 38 and 66% anatomical sites.

MATERIALS AND METHODS

Sample Population

Cadaveric tibiae from 10 donors (6 male, 4 female, age 37 +/− 8 years of age) were either donated or purchased from the Musculoskeletal Transplant Foundation (Edison, NJ) and the National Disease Research Interchange (Philadelphia, PA). These samples represent the contralateral limb of a subset of the individuals utilized by Tommasini et al. (2005, 2007, 2008). None of the cadavers had a medical history showing a disease or condition that would affect the skeleton.

Sectioning and Imaging Methods

Two 2.5 mm thick cross sections and one 5 mm thick cross section were removed from each tibia at both the 38% and the 66% sites along the tibial length, measured from the distal end of the bone (Fig. 1), using a diamond coated band saw (Exakt Technologies; Oklahoma City, OK). The first of the 2.5 mm sections was imaged using pQCT (XCT 2000; StratecMedizintechnik, Pforzheim, Germany) to calculate robustness, which was defined as total cross-sectional area, Tt.Ar, divided by total tibial length, Le (Tt.Ar/Le; Fig. 1). Tibial length was measured as the average distance between the middle of the talar trochlear facet and the medial and lateral proximal condyles, as described previously (Tommasini et al., 2007). These cross-sections were then ashed following the methods of Tommasini et al. (2008). The second set of 2.5 mm cross-sections was further sectioned into 6 radial wedges (see Fig. 1) before being imaged by μCT, as described below. This step was necessary in order to obtain μCT images of adequate resolution to accurately quantify vascular pores within the bone cortex. Imaging the cross-section as a single block at lower resolution would result in excessive imaging times and added noise in the resultant images, decreasing our ability to detect pores adequately. After μCT imaging, wedges were ashed following the methods of Tommasini et al. (2008).

The 5 mm thick cross-section was cleaned of soft-tissue, defatted, and embedded in polymethylmethacrylate using methods described previously (Goldman et al., 2003a, b; Tommasini et al., 2008). Blocks were ground smooth using 1200 grit sandpaper on the surface of the block closest to the 2.5 mm block used for μCT analysis. The polished surface was adhered to a plastic slide, cut to ~300 μm thickness using a Buehler Isomet 1000 saw and ground/polished to ~100 μm thickness using a series of graded sandpapers (ending at 1200 grit; Goldman et al., 2009). Specimens were cover-slipped using ethylene glycol prior to imaging with transmitted and polarized light microscopy.

μCT Imaging and Image Analysis

Wedges were imaged using a Skyscan 1172 μCT system (Bruker Corp., Kontich, Belgium) at 4.8 μm voxel size, 1 mm Aluminum filter, 0.5° rotation step and frame averaging of 10. This resolution captured vascular spaces (including primary vascular canals, Haversian canals, Volkmann's canals, and resorption bays) while excluding osteocyte lacunae. Blocks were reconstructed using NRecon (Bruker Corp., Kontich, Belgium) and digitally aligned using Dataviewer (Bruker Corp., Kontich, Belgium). Cortical regions of each wedge were hand selected and a series of noise reduction steps was performed by applying a 1-pixel median filter to the image stack using ImageJ, followed by a series of de-speckling and morphological processing steps (opening) using the

manufacturer's software. These procedures were standardized for all blocks. However, an additional processing step was added to some samples if visual inspection showed lingering noise. A region of interest (ROI) was manually selected to exclude cancellous bone (defined visually as regions with greater than ~50% porosity). The final ROI was shrink-wrapped to the very edge of the bone and then eroded by 2 pixels to remove edge artifacts. Finally, for the purposes of our wedge analysis (used to determine whole cross-section relationships between porosity and robustness) all pores with a diameter larger than 300 μm were excluded, as those pores were unlikely to reflect Haversian or Volkmann's canals that relate to the intracortical remodeling process. Total tissue volume (Tt.V) and total canal volume (Tt.Ca.V) were measured. Porosity (Ct.Po, %) was calculated as canal volume normalized by total tissue-volume. Data from each of the six wedges were combined to generate an average Ct.Po for each cross-section.

Three regions of interest (ROIs) were extracted from each 3D wedge dataset, provided that the wedge was wide enough along its center-line to accommodate three 1 mm^3 boxes. ROI selection was automated by a MATLAB program (MathWorks, Natick, MA) that chose the periosteal and the endosteal ROIs such that they were as close to the edges of the bones as possible, while staying completely within the bone. The midcortex ROI was spaced halfway between the periosteal ROI and the endosteal ROI when the cortical thickness was great enough to allow all 3 ROIs without any overlap. If the cortical thickness did not allow for 3 ROIs, the midcortex ROI was chosen to be a set distance from the edge of the periosteal ROI and no endosteal ROI was extracted.

Light Microscopy and Histomorphometric Measurements

Each histological section was imaged using transmitted light microscopy with and without circularly polarized light filters. Images were collected using a Zeiss Axioplan 40 (Wexlar, Germany) transmitted light microscope fitted with a motorized X, Y, and Z stages with output via an Optronix digital CCD camera to MBF Bioscience's Virtual Slice software program (South Burlington, Vt). Individual images were montaged to generate a single high-resolution image of the entire cross-section (pixel size = 1.44 μm). Paired montages were aligned to one another, then twelve 1 × 1 mm^2 ROI's were extracted (Fig. 1) using an automated MATLAB routine (MathWorks, Natick, MA), following the same criteria used to extract the μCT ROIs (see above). Primary bone area, secondary bone area, primary pore area (Po.Ar), and secondary Po.Ar were hand traced for each ROI. Primary bone was defined as any nonlamellar tissue as well as all circumferential lamellar bone and primary osteons. Secondary tissue was defined as the remaining bone area, including secondary osteons, osteon fragments, secondary interstitial bone, and the area of associated pores. The % secondary tissue measurement, therefore, included all bone tissue and porosity that resulted from the intracortical remodeling processes.

Osteons were chosen for measurement based on criteria from previous studies (Pfeiffer, 1980; Stout and Paine, 1994). Specifically, in order for an osteon (and its Haversian canal) to be measured, the Haversian canal needed to be completely located within the area of interest; it could have a maximum diameter no more than twice the minimum diameter, and must have had 90% of its perimeter and the entire Haversian canal visible. In the case of eccentric or drifting osteons, a symmetrical measure of the osteon was taken by following the most external lamella on the nondrifting side of the osteon around, if a clear boundary could be discerned. By designing our methods in this way, we were able to count eccentric osteons, and include the measurement of their Po.Ars, but eliminated the uncertainty of defining the area of the drifting portion of the osteon. In practice, due to the fact that these were unstained sections, it was often difficult to demarcate the edge of these osteons and differentiate them accurately from adjacent interstitial bone. Thus, including this tissue area would have led to excess variability in our dataset. Area measurements included Osteon Area (On.Ar) and Po.Ar. Osteon Fragment Number (Os.Fr.N) includes osteons with <90% of their Haversian canal visible, but >0%. Osteon Population Density (OPD) was calculated as the number of intact + fragmentary osteons in the ROI. All measurements were obtained by hand tracing using Adobe Photoshop (San Jose, CA) and a Wacom digitizing tablet (Wacom Technology, Vancouver, WA).

Although periosteal and endosteal ROIs were obtained (for both μCT and LM datasets), only midcortex ROI data were analyzed for this study. The midcortex was most likely to contain numerous osteons that were formed as part of the BMU-based remodeling process. The periosteal ROI contained less secondary osteonal tissue and more primary tissue that formed during growth as part of the modeling process (Enlow, 1962) while the endosteal ROI contained numerous subendosteal pores likely representing areas of infilled trabeculae, or as a result of medullary expansion (Enlow, 1962), rather than from BMU-based remodeling.

Statistical Analysis

Correlations between measures of BMU-based remodeling and bone robustness were determined by linear regression analysis. For each variable, data were averaged from multiple ROIs to generate a dataset representative of the entire cross-section. Because several of the histological measures may contribute to porosity simultaneously, a multivariate analysis was also conducted to establish the relative contributions of measures related to activation (OPD), resorption (osteon size), and formation [% infilling = (osteon size − pore size)/osteon size]. To determine how the histological measures varied along the tibia, the histological measures at the 38% and 66% sites were regressed against each other and the slope and y-intercept were compared to an ideal line (slope = 0, y-intercept = 0) by ANCOVA.

RESULTS

Interactions Among Porosity, Ash Content, and Robustness

Figure 2 illustrates the dramatic visual difference in porosity between a slender and a robust individual at the 66% site. Linear regression analysis (Fig. 3a,b) showed that porosity increased with robustness at the 66% site ($R^2 = 0.65$, $P < 0.005$); however, no correlation

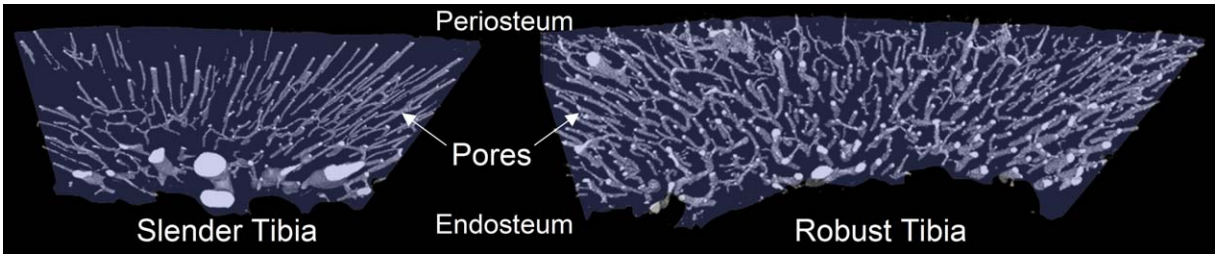

Fig. 2. Rendered microCT images illustrating the differences in porosity (number, density, and size of pores) between a slender (left) and robust (right) bone. The regions of interest were taken from the antero-medial sector and both were scaled similarly.

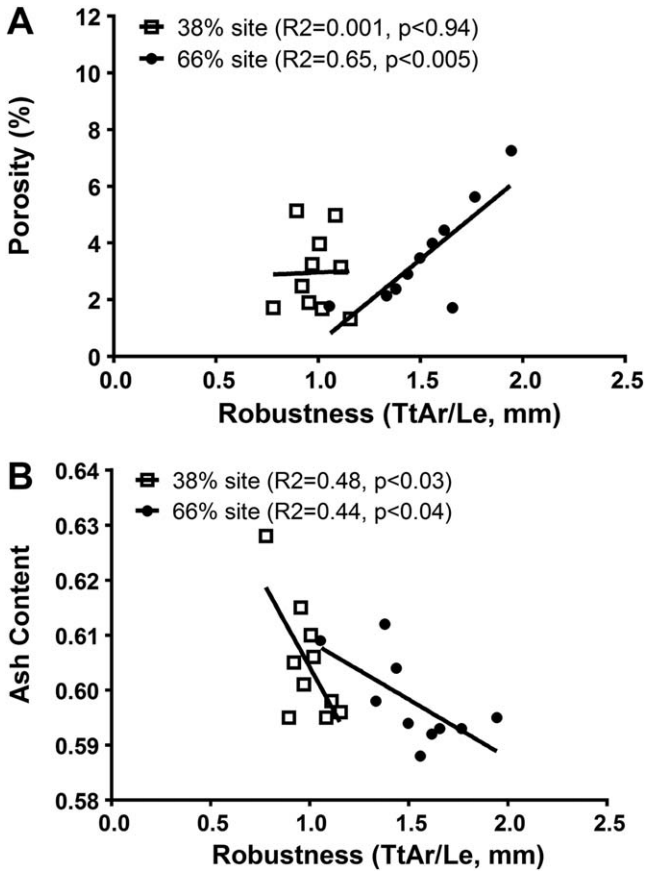

Fig. 3. Linear regression analysis was conducted to test for associations between robustness and (**a**) porosity and (**b**) ash content measured at the 38 and 66% sites. Porosity was measured by microCT across the entire sextant, and the values averaged across the six wedges.

was found at the 38% site ($R^2 = 0.001$, $P < 0.94$). Ash content decreased with robustness at both the 38% ($R^2 = 0.48$, $P < 0.03$) and 66% sites ($R^2 = 0.44$, $P < 0.04$).

To better understand why the correlation between robustness and porosity was not significant at the 38% site, we examined the relationship between measures obtained at 38% and those obtained at 66%. The coefficient of variation (COV = standard deviation/mean) in robustness at the 66% site was 44% greater than the COV at the 38% site (COV 66% = 16.2% vs. COV 38% = 11.3%). The differences in variation are reflected in a bivariate plot of robustness measured at the two sites (Fig. 4a).

Given these site-specific differences in the degree to which robustness varies among individuals, we tested whether robustness-specific differences in porosity and ash content observed at 66% were consistent along the length of the bone (Fig. 4b,c). Porosity at 38% correlated significantly with the porosity at 66% ($R^2 = 0.95$, $P < 0.0001$). The slope of this line was significantly different than 1 ($P < 0.0008$, ANCOVA), indicating that although they are highly correlated, there is greater porosity at 66% relative to 38%. This was confirmed by a paired t-test ($P = 0.007$). Likewise, ash content at the 38% site correlated positively with ash content at 66% ($R^2 = 0.55$, $P < 0.01$). The y-intercept of this regression was significantly different from 0 ($P < 0.007$, ANCOVA), indicating that the ash fraction was lower at the 66% site relative to the 38% site. This was confirmed by a paired t-test ($P = 0.01$).

Porosity as a Reflection of the Intracortical Remodeling Process

To understand how variation in porosity is related to the BMU-based remodeling process, we conducted a series of regression analyses among histological variables that reflect activation (OPD), resorption (On.Ar.), and formation (% infilling). We also examined additional variables resulting from the BMU-based remodeling process such as % secondary bone and pore size (Po.Ar.). As discussed above, we focused our histomorphometric analysis on the midcortical region because bone within this region is largely remodeled, and pores largely reflect Haversian canals. In addition, a validation study demonstrated that porosity measurements from a 1 mm midcortex ROI were highly correlated with the porosity of the whole cross-section ($R^2 = 0.89$ at 38%, $P < 0.001$; $R^2 = 0.91$ at 66%, $P < 0.001$, data not shown), suggesting that the ROIs included in the analysis below are representative of the dynamics occurring across sections.

Bivariate plots of porosity versus each of our histological variables (Fig. 5) demonstrated that average On.Ar. ($R^2 = 0.67$, $P < 0.004$), average Po.Ar. ($R^2 = 0.56$, $P < 0.01$), and OPD ($R^2 = 0.19$, $P < 0.21$) correlated positively with porosity. The % secondary bone also correlated positively with porosity ($R^2 = 0.32$, $P < 0.09$) but this relationship improved, as expected, when modeled as a one-phase exponential association ($R^2 = 0.44$). The % infilling correlated negatively with porosity ($R^2 = 0.40$,

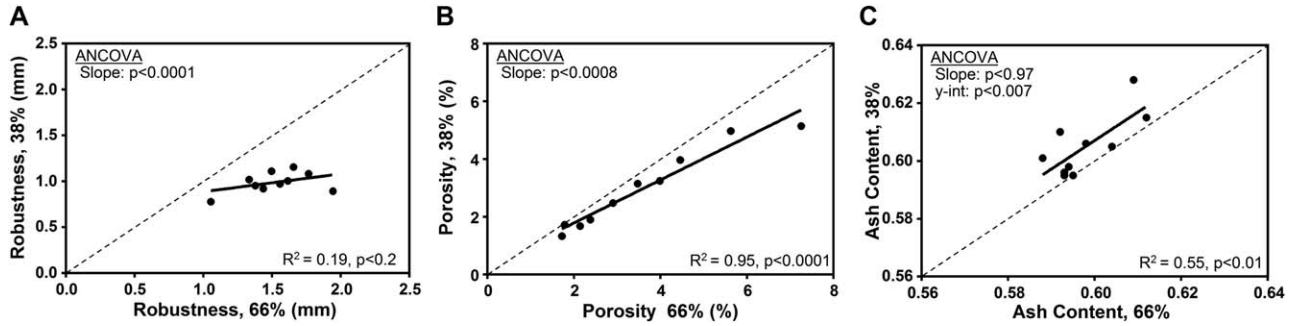

Fig. 4. Linear regression analysis was conducted to test for associations between the 38 and 66% anatomical sites for measures of (**a**) robustness, (**b**) porosity, and (**c**) ash content. The dashed line has a slope of 1.

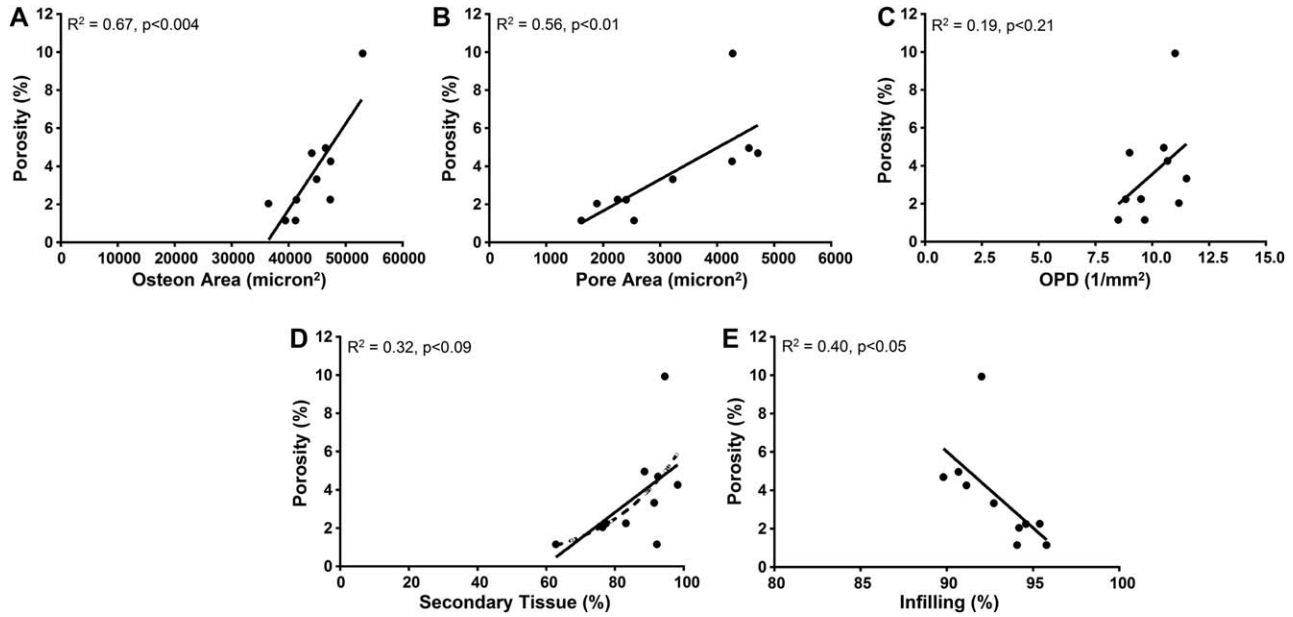

Fig. 5. Linear regression analysis was conducted to test for associations between porosity and (**a**) average On.Ar, (**b**) average Po.Ar, (**c**) OPD, (**d**) % secondary tissue, and (**e**) % infilling. The histomorphometric data shown here were measured at the 66% anatomical site.

$P < 0.05$). Multivariate analysis provided additional insight into the relative contributions of these remodeling parameters to porosity. Specifically, measures of activation frequency (OPD), Resorption (On Ar.), and Formation (% infill) all contributed significantly to the variation in the porosity of the midcortex ROI, together accounting for ~66% of the variation in porosity ($P < 0.02$). On.Ar was the only significant single term. In sum, greater porosity was accounted for by having larger osteons, more numerous osteons, and less infilling. The larger osteons combined with reduced infilling resulted in larger pore sizes.

Histological Parameters and Robustness

At the 66% site, linear regression analysis showed significant positive correlations between total Po.Ar ($R^2 = 0.53$, $P < 0.02$) and % secondary bone ($R^2 = 0.68$, $P < 0.004$) and robustness. In addition, total On.Ar ($R^2 = 0.42$, $P < 0.04$), average On.Ar. ($R^2 = 0.30$, $P < 0.1$), average Po.Ar. ($R^2 = 0.30$, $P < 0.1$), OPD ($R^2 = 0.32$, $P < 0.09$) all showed trends towards a positive correlation with robustness. % infilling tended to correlate negatively with robustness ($R^2 = 0.22$, $P < 0.17$). In sum, at the 66% site, robust bones tended to have, on average, larger and more numerous osteons, with less infilling, resulting in bigger pores and more secondary bone area. No significant results, or notable trends, were seen at the 38% site.

Next, we took a regional approach to determine whether there were some cortices at the 66% site where relationships with robustness were stronger than others. On its own, the posterior ROI had the highest correlations with robustness, followed by postero-medial and postero-lateral cortices. Linear regression analysis (Fig. 6) considering only the posterior half of the bone

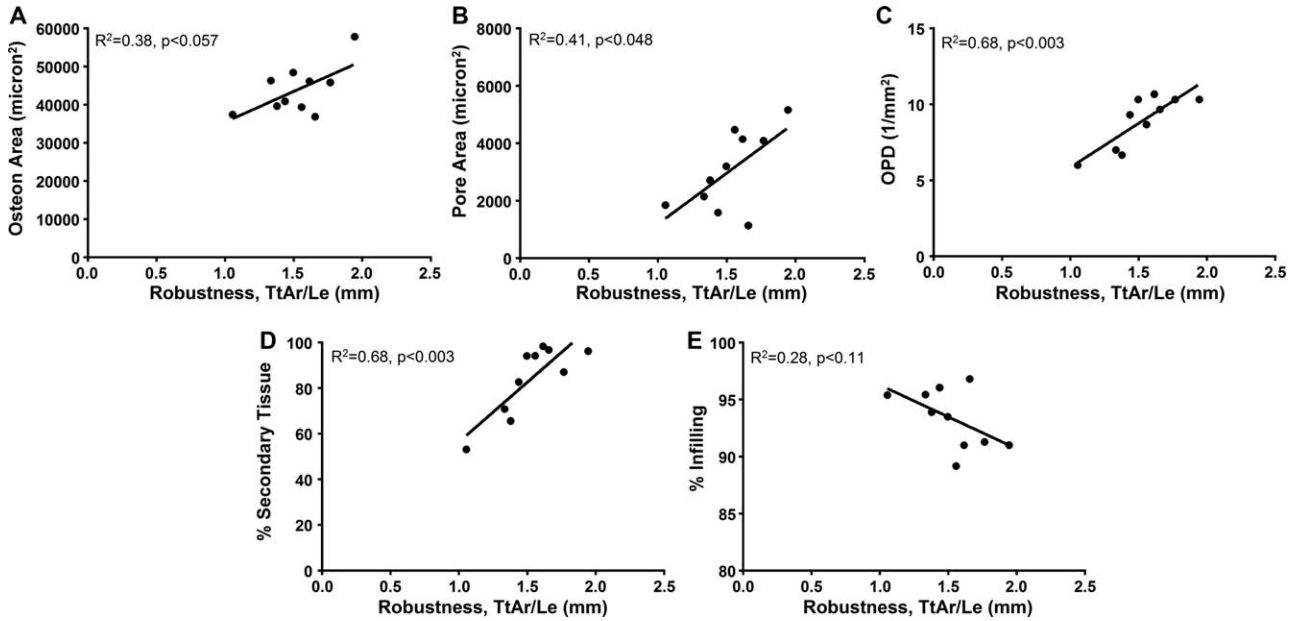

Fig. 6. Linear regression analysis was conducted to test for associations between robustness and (**a**) average On.Ar, (**b**) average Po.Ar, (**c**) OPD, (**d**) % secondary tissue, and (**e**) % infilling. The histomorphometric data shown here were measured at the 66% anatomical site and averaged over the three posterior sextants only.

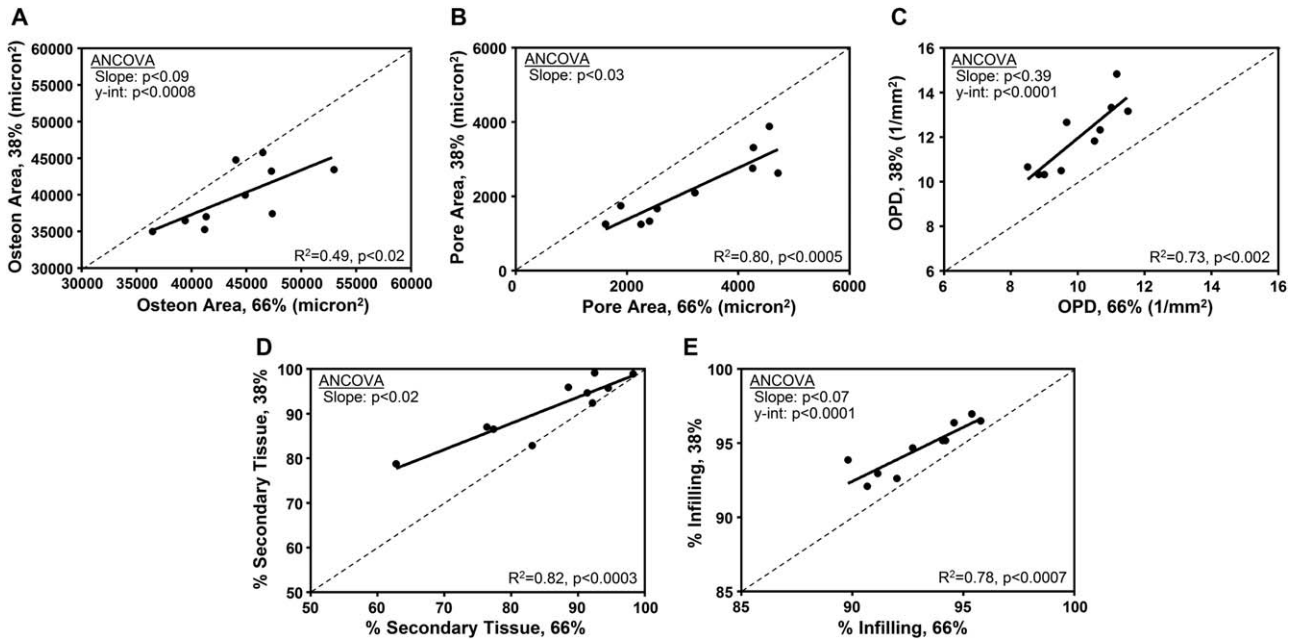

Fig. 7. Linear regression analysis was conducted to test for associations between the 38 and 66% anatomical sites for measures of (**a**) average On.Ar, (**b**) average Po.Ar, (**c**) OPD, (**d**) % secondary tissue, and (**e**) % infilling. The dashed line has a slope of 1.

showed positive correlations between total On.Ar ($R^2 = 0.60$, $P < 0.009$; not shown), average On.Ar. (Fig. 6a; $R^2 = 0.38$, $P < 0.057$), total Po.Ar ($R^2 = 0.59$, $P < 0.01$; not shown), average Po.Ar. (Fig. 6b; $R^2 = 0.41$, $P < 0.048$), and OPD (Fig. 6c; $R^2 = 0.68$, $P < 0.003$) and % secondary bone (Fig. 6d; $R^2 = 0.68$, $P < 0.003$). % infilling tended to correlate negatively with robustness (Fig. 6e; $R^2 = 0.28$, $P < 0.11$).

Similar to the analysis conducted with ash content and porosity, we wanted to know whether these remodeling parameters were consistent between the 38% and 66% sites. Regression analysis showed that On.Ar.

($R^2 = 0.49$, $P < 0.02$), Po.Ar. ($R^2 = 0.80$, $P < 0.0005$), OPD ($R^2 = 0.73$, $P < 0.002$), % secondary bone ($R^2 = 0.82$, $P < 0.0003$), and % infilling ($R^2 = 0.78$, $P < 0.0007$) were positively correlated between the two sites (Fig. 7).

Based on ANCOVA and paired t-tests, the 38% site showed larger total On.Ar (ANCOVA slope, $P < 0.038$; paired t-test, $P < 0.01$; not shown) and more secondary tissue (Fig. 7c; ANCOVA slope, $P < 0.02$; paired t-test, $P < 0.01$), but no difference in the total Po.Ar between sites (ANCOVA slope, $P < 0.7$, y-intercept, $P < 0.4$; paired t-test = 0.4). This resulted from the 38% site having, on average, smaller sized osteons (Fig. 7a; ANCOVA slope, $P < 0.09$; y-intercept, $P < 0.0008$; paired t-test, $P < 0.004$), more numerous osteons (OPD; Fig. 7c; ANCOVA slope, $P < 0.39$; y-intercept = 0.0001, paired t-test, $P < 0.0001$), and smaller average Po.Ars (Fig. 7b; ANCOVA slope, $P < 0.03$; paired t-test = 0.0003), resulting from greater % infilling (Fig. 7e; ANCOVA slope, $P < 0.07$; y-intercept, $P < 0.0001$; t-test, $P < 0.001$).

DISCUSSION

BMU-based remodeling plays a critical role in mechanical homeostasis and skeletal fragility, because it defines porosity, matrix composition, tissue-level mechanical properties, and age-related bone loss (Frost, 1987; Zebaze et al., 2010). The results of the current study confirmed those of our previous work (Jepsen et al., 2011), demonstrating a significant positive relationship between porosity and robustness and a significant negative relationship between ash content and robustness at the 66% site of the human tibia. This outcome supports our hypothesis that more slender bones increase ash content and decrease porosity to increase tissue level stiffness, whereas more robust bones increase porosity to minimize mass. The highly consistent patterns we found across skeletal sites could also be explained by the natural variation in robustness. Finally, we demonstrated a significant association between our porosity data and standard histomorphometric measures of bone remodeling and between these measures and robustness, confirming that the association between intracortical porosity and robustness (Jepsen et al., 2011) was mediated by BMU-based remodeling.

Intrabone Variation

Our results demonstrated a significant positive correlation between porosity and robustness and a significant negative correlation between ash content and robustness at the 66% tibial site but not at the 38% site. The lack of significance between robustness and porosity and between robustness and ash content at the 38% site does not invalidate the concept that slender bones are constructed differently than robust bones. Rather, our results showed highly consistent patterns of variation between sites, suggesting that both sites respond to the same global effects and demonstrate a similar character at the whole bone level. In other words, if porosity is low at one site, it will also tend to be low at another site. Prior work concerning the effect of robustness on bone properties did not differentiate among sites (Tommasini et al., 2008) or presented data only from a single site (Jepsen et al., 2011).

An explanation for the lack of significant relationships with robustness at the 38% site may relate to the fluted shape of the tibia. The proximal tibia (66% site) is a more robust site relative to the distal tibia (38%), with the latter also showing much less variability in robustness. Arguably, the lack of relationship with robustness at the 38% site could be due to the fact that all bones were so similarly slender that differences owing to robustness could not be detected. Further, as bones at the 38% site tend to be at the more slender end of the variability spectrum, there may be constraints on minimal vascular support and limitations on the maximum mineralization of the tissue (to avoid becoming too brittle), resulting in a lower limit to the remodeling response. This may limit our ability to detect relationships when only the slender end of the spectrum is represented. However, in a more robust cross-section—only represented in the 66% samples—there would be more natural selection pressure to extensively increase porosity (through intracortical remodeling) to decrease mass. In this sense, this study also presents a cautionary note to future investigations looking at these associations that multiple sites, which exhibit ample variation in robustness, be used to study these relationships.

Although limited variation in robustness might explain the lack of correlation seen at the 38% site, the mechanical loading environment at the distal tibia should also be considered. The distal tibia has been hypothesized to experience higher tissue-level strains compared to the more proximal sites (Milgrom et al., 1989; Ekenman et al., 1998). Moreover, limbs tend to taper distally so that mass (skeletal and muscle) tends to be located closer to the axis of rotation of the body. This reduces the energy cost of locomotion (Alexander, 1998; Hildebrand and Goslow, 1998; Dellanini et al., 2003). Lieberman et al. (2003) suggested that the more slender geometry of the distal elements combined with higher resultant strains would result in greater accumulation of microdamage, and thus higher remodeling rates in response to normal loading conditions. Extrapolating this to a comparison of microstructural measures between the proximal and distal tibial sites, one would expect higher remodeling rates at the distal (38%) site compared to the proximal (66%) site. We found that the 38% site had higher average OPD and more secondary tissue, which is consistent with expectations that the 38% site may sustain more microdamage and thus initiate a larger number of remodeling events. However, this relationship is opposite to what we would predict based solely on the relationship between robustness and remodeling observed from regressions at the 66% site. However, the 38% site did show smaller average On.Ar, average Po.Ar and greater infilling, which is consistent with the relationship between robustness and remodeling observed from regressions at the 66% site. Perhaps the lack of correlation between robustness and remodeling at the distal site may be revealing new insights into competing constraints on remodeling, balancing local needs (e.g., limiting microdamage, vascular support, etc.) with adaptive processes associated with the natural variation in bone morphology (e.g., the need to reduce porosity to increase tissue stiffness). A previous study by Ural and Vashishth (2006) demonstrated site specific relationships between microstructure and geometry at the more distal tibial diaphysis, but not at the more

proximal tibial site. The authors explained this finding relative to local mechanical responses to strain levels and muscle attachments. The authors did not analyze their data relative to a robustness measure, but it is possible that incorporating the robustness variable into their analysis could have provided additional explanations for their findings.

Site-specific variability may relate to other global factors as well. Studies have shown that more distal sites experience greater increases in bone mass relative to more proximal sites during growth in response to exercise (Iwamoto et al., 1999; Turner, 1999; Hamrick et al., 2006). The site-specificity of bone formation, hypothesized by Turner to be related to fluid pressure gradients, may be superimposed upon the variation related to robustness, and should be investigated as an additional contributor to the variation in geometry and microstructure at distal sites. Skedros (2012) cautioned that the loading in the tibia is relatively complex, with torsion along with combined bending and compression, with torsion increasing towards the distal end of the tibia. Differences in loading patterns between proximal and distal tibia could explain some of our results, and may be helpful in interpreting differences in regional variability around the cortex at each site. Future work should address these competing factors using larger cadaveric datasets to better understand the associations between BMU-based remodeling and global morphology.

Porosity as a Reflection of the Intracortical Remodeling Process

We analyzed the relationships between porosity and BMU-based remodeling by studying the midcortical region, because bone located deep within the cortex of the adult will tend to be largely remodeled (Pfeiffer et al., 1995; Thomas et al., 2005) and pores were most likely to have been formed through the BMU-based remodeling process. This has been confirmed in our study based on the associations between porosity and BMU-based parameters discussed below. The periosteal cortex, however, would likely contain higher proportions of primary tissue and pores as part of the bone modeling process that occurs during cortical expansion and drift (Enlow, 1962; McFarlin et al., 2008; Goldman et al., 2009). The endosteal region of the cortex often contains larger pores that may represent areas of infilled trabeculae (Enlow, 1976) rather than BMU-based remodeling, or that may reflect the confluence of resorption bays resulting from repeated activation events that are not followed by bone formation, and that have been associated with age-related subendocortical bone loss (Bell et al., 2001).

We hypothesized at the outset of this study that modulation of mineralization and porosity could be accomplished through the BMU-based intracortical remodeling process. To address this question, we utilized standard static histomorphometric measures of BMU-based remodeling (Stout and Crowder, 2012), which is appropriate for analysis of cadaveric tissue, to study the relationship between these metrics and bone porosity in the context of bone robustness. We chose a 1 mm ROI for our analysis, as a sampling size of that magnitude has been shown in previous studies to be representative of the histological variation within the subperiosteal region of the cortex (Iwaniec and Crenshaw, 1998). Our validation study confirmed that porosity measurements from a 1 mm mid-cortex ROI were highly correlated with the porosity of the whole wedge. In support of our hypothesis, we found associations between porosity and a number of standard histological variables that reflect the A,R,F sequence of the remodeling process, specifically those related to Resorption (Osteon Size) and Formation (% infilling). The association between porosity and activation (OPD) was not significant. In the multivariate regression, osteon size was the dominant trait contributing to the variation in porosity. In summary, we found that greater porosity was accounted for by having larger, slightly more numerous osteons, and less infilling. The larger osteons combined with reduced infilling may also help explain the strong positive correlation between Po.Ar and porosity (Fig. 5). We also demonstrated a positive relationship between % secondary bone and porosity. This was expected because Haversian remodeling results in increased numbers of pores in the form of Haversian canals, as well as increased Po.Ar due to accumulating canals formed by remodeling events (Currey, 1964; Kerley, 1965; Jowsey, 1966; Martin et al., 1980; Thompson, 1980). This relationship appears to be nonlinear, likely because some regions of the cortex reach a level of 100% remodeled tissue, yet these same areas would continue to accumulate pores.

Although this study focused specifically on the correlations between average trait values and robustness, we fully recognize the significant variation underlying these mean values. Regional variation in porosity and histological parameters within a cross-section have been shown to relate to local strain (Martin et al., 1980; Lazenby, 1986; Burr et al., 1990; Feik et al., 1997), patterns of growth and development (Pearson and Lieberman, 2004; Main, 2007; McFarlin et al., 2008; Goldman et al., 2009), nutritional factors (Ericksen, 1980; Thompson and Gunness-Hey, 1981; Stout and Lueck, 1995; Seibel, 2002), metabolic disease (Eriksen et al., 1989; Mosekilde, 2008), and chronological and skeletal ages (Epker and Frost, 1966; Martin et al., 1980; Frost, 1987; Stout and Paine, 1994) and sex (Kerley, 1965; Frost, 1987; Burr et al., 1990; Cho et al., 2006). These are all important factors to consider in interpreting histological variation. However, analyzing our data as we did brings the opportunity to study this variability in the context of competing influences on bone architecture including global factors related to bone size/external morphology as well as these other factors. We sought to understand this global relationship first, and then with subsequent studies, using larger numbers of samples and multiple skeletal sites, to begin to tease apart the roles of other competing factors.

Histological Parameters and Robustness

Based on our finding that more slender bones tend to be less porous than robust bones and on the association demonstrated between porosity and histomorphometric parameters of intracortical remodeling, we examined the relationship between these histological parameters and robustness. We found significant positive correlations between robustness and average pore size and % secondary bone, and positive trends between robustness and total On.Ar, average On.Ar, total Po.Ar, and OPD. Percent infilling tended to correlate negatively with

robustness. In summary, robust bones tended to have larger and more numerous osteons with less infilling, resulting in bigger pores and more secondary bone area. When these associations were limited to the posterior half of the bone, nearly all relationships were found to be significant. We suspect that the inclusion of the anterior portion of the bone, which includes a large muscle attachment site, may obscure some of these associations when averaged across all sites. In addition, these associations may be affected by local mechanical loading due to ambulation.

The associations between intracortical remodeling, bone cross-sectional morphology (Martin et al., 1980; Lazenby, 1986; Burr et al., 1990; Walker et al., 1994; Bjornerem et al., 2013) and mechanical loading (Bouvier and Hylander, 1981; Frost, 1987; Skedros et al., 2004; Goldman et al., 2005; Thomas et al., 2005; van Oers et al., 2008a,b; Schlecht et al., 2012) are well established, but have generally been examined at a local level, focusing on how local strain variation in the cortex may relate to remodeling rates (and hence osteon size and OPD). Thomas et al. (2005), for instance, found that analyzing porosity variability by a measure of cross-sectional geometry (ratio of medullary area to total subperiosteal area) explained the variability in their adult sample better than chronological age, again suggesting that porosity (and hence remodeling parameters) is related to bone size. Ural and Vashishth (2006) found correlations between geometry and microstructure at the proximal mid-diaphysis of the tibia but not in the distal aspect. They interpreted this result in the context of site-specific differences in muscle mass and strength, and to higher strain levels at the distal site. As discussed above, the authors did not analyze their data relative to a robustness measure, but their results are likely consistent with our hypothesized relationship. Thus, the relationship demonstrated in this study between robustness and histological measures of remodeling has not previously been shown, and would suggest that there is a biological pathway associated with robustness that regulates intracortical remodeling in the context of how the complex adaptive nature of the skeletal system interfaces with the natural variation in bone robustness (Jepsen et al., 2011). This level of regulation would be superimposed upon variability in remodeling rates that relate to local variation in mechanical loading around the cortex.

Establishing the biological basis for these associations is not simple. However, our results are entirely consistent with data on the incidence of mechanical forces and the association between BMU-based metrics and cortical area. Traditionally, histomorphometric parameters have been related to the distribution of local mechanical forces as discussed above. However, we also need to consider the magnitude of the forces, which vary predictably relative to the natural variation in robustness. As reported previously (Jepsen et al., 2011, 2013), the complex adaptive nature of the skeletal system adjusts tissue mineral density (TMD) relative to robustness, presumably to offset the smaller cross sectional size by increasing tissue stiffness. Despite the significant associations shown, there are limitations in the degree to which bone cells can adjust TMD, resulting in slender bones being about 2× less stiff for body size compared with robust bones. Given that slender bones may experience greater peak strains than robust bones, the association between intracortical remodeling and robustness is consistent with the mechanostat theory (Frost, 1987). This theory postulates that higher strains below a damage threshold (i.e., slender bones) suppress remodeling to increase tissue-modulus whereas low strains stimulate remodeling to reduce mass (i.e., robust bones). Our finding that slender bones had significantly smaller osteons than more robust bones, appears to support this concept and there are additional studies that support this as well. van Oers et al. (2008a,b) computationally explained a negative correlation between osteon size and tissue strain and other studies have demonstrated such correlations experimentally (Skedros et al., 1997; Britz et al., 2009). Skedros (2012), on the other hand, cautions that osteon size may be unreliable for interpreting load history, as studies have been inconsistent [e.g., Mason et al. (1995) and Skedros et al. (2009) demonstrated no relationship]. Alternative explanations for our results include considering that slender bones also have smaller cortical areas on an absolute basis compared to robust bones, and Frost (1987) found smaller osteons in bones with smaller cortical areas when examined across skeletal sites. Further, other studies have explored the role of weight bearing in modulating osteon size (Britz et al., 2009), as well as complexities in interpreting findings of decreasing osteon size with age (Currey, 1964; Takahashi et al., 1965; Britz et al., 2009) which may relate to decreasing propensities of drifting osteons and increased circularity with age (Currey, 1964; Britz et al., 2009). While our osteon measurement protocol eliminated the inclusion of eccentrically placed tissue in drifting osteons, including additional histomorphometric variables such as quantifying eccentric osteons, and measuring osteon diameter (On.Dm) or osteon circularity (On.Cr.) may help provide additional insight into the relationship between remodeling parameters, including porosity, and skeletal robustness.

As discussed above, we also found significant correlations between ash content and robustness, and this relationship can be tied, in part, to the remodeling process. In this study, we were able to demonstrate associations between porosity and measures of remodeling, but we still do not know how the BMU-based system affects the relationship between mineralization and robustness. The negative correlation between mineralization and robustness has been observed in mice, which do not have a BMU-based remodeling like humans, suggesting that part of the differential mineralization among individuals may result from the way the extracellular matrix is mineralized after deposition (Jepsen et al., 2007; Courtland et al., 2008). These observations in mice, however, do not rule out the contribution of variable remodeling on mineral content in human bone. Mineralization has been shown to vary with respect to remodeling status (Meunier and Boivin, 1997; Hernandez, 2008), as a high remodeling rate leads to a high amount of bone turnover, and newly formed bone has a lower mineralization level. Thus, variability in mineralization could result from direct effects on osteoblasts (e.g., osteoblasts in slender bones produce a more mineralized matrix), or as a byproduct of tissue age owing to remodeling rate. Further research utilizing more sensitive and localized measures of tissue mineralization (e.g., using Quantitative Backscattered Electron Microscopy or Raman/FTIR

measures of mineral to matrix ratio) are required to determine whether the mineralization differences seen can be fully explained by differences in remodeling rate compared with differences in the mineralization process between slender and robust bones. Further research in human cadaveric tissue is needed to better refine these associations to identify an appropriate animal model.

Limitations and Future Work

This study represents a first attempt to establish associations between the natural variation in bone size (robustness) and indicators of bone remodeling, looking at multiple ROIs at two sites and showing highly consistent associations in nearly all porosity, composition, and remodeling parameters between the 38% and 66% sites. The data were collected in a blinded manner, providing confidence in these associations. The significant correlations justify the need to expand this type of approach to a bigger dataset and to test for effects of sex, ethnicity, and anatomical site. Although we could not test for sex-specific effects due to our small sample size, our female samples did tend to be more slender than the males, as expected. If in a larger sample a significant sex difference were to be shown, it may be possible to explain this difference in the context of robustness. We also purposefully limited the age range of the study sample so that we could examine these relationships in a young adult sample, as the effects of aging might obscure these associations. However, in future studies it will be important to understand how existing population variability in morphological parameters such as robustness may differentially affect aging and the response to prophylactic treatments to address bone health.

Although we were able to detect associations between BMU-based remodeling and robustness, an expanded sample would allow us to more closely examine which aspects of the A,R,F sequence contributed most to this relationship. Our study has already highlighted significant patterned regional variability: associations shown at the 66% site but not the 38% site and stronger correlations between histomorphometric variables posteriorly versus anteriorly. This information will allow us to target specific areas of the cortex in future studies, and thereby reduce some of the expense involved in creating a collection of young adult cadavers and the time for obtaining laborious histomorphometric data sets. Given that the modeling process provides the crucial mechanism for establishing morphological variation to begin with, a similar focus on links between robustness and bone modeling, using a regional approach to examine variability, is also needed. An approach considering both modeling and remodeling and their "division of labor" in the establishment and modification of bone properties may provide new insight into morphological and material property adaptations in the skeleton (Skedros et al., 2013) and help tease apart the effects of global and local signals that may regulate these processes.

CONCLUSIONS

In summary, the data showed that intracortical, BMU-based remodeling varies significantly with the natural variation in bone robustness. This association is consistent with work by us (Tommasini et al., 2008) and others (Thomas et al., 2006; Ural and Vashishth, 2006) and with data showing suppressed age-related bone loss in slender but not robust femoral cortices (Epelboym et al., 2012). These studies suggest that local regulation of remodeling (Verborgt et al., 2000; Kennedy et al., 2012) may be further modulated by a global signal associated with robustness. Molecular regulation of this global signal is unknown, but is likely mediated through differential strains sensed by osteocytes (van Oers et al., 2008b). This global regulation of remodeling appears to modulate porosity and possibly mineralization to maximize tissue-modulus and whole bone strength in slender bones and to minimize mass in robust bones. The association between remodeling and robustness may be critical for mechanical homeostasis, but may increase bone brittleness for certain individuals. Thus, not all bones are constructed in the same way, and part of the interindividual variation in microstructure and composition can be explained by the natural variation in morphological traits like robustness.

ACKNOWLEDGEMENTS

The opinions or assertions contained herein are the private views of the authors and are not to be construed as official or as reflecting the views of the U.S. Army or the Department of Defense. The content is solely the responsibility of the authors and does not necessarily represent the official views of the National Institutes of Health**.** The authors thank Alka Basnet (Drexel), Mathew Chin, Ashley Campbell, and Lindsey Kent (Drexelmed) for assistance with various stages of specimen preparation and imaging, and Jerrald Chen (Drexelmed) who programmed the MATLAB Routines used to extract regions of interest from 2D and 3D datasets.

LITERATURE CITED

Alexander RM. 1998. Muscle geometry. J Physiol 512 (Pt 2):315.

Bell KL, Loveridge N, Reeve J, Thomas CD, Feik SA, Clement JG. 2001. Super-osteons (remodeling clusters) in the cortex of the femoral shaft: influence of age and gender. Anat Rec 264:378–386.

Bjornerem A, Bui QM, Ghasem-Zadeh A, Hopper JL, Zebaze R, Seeman E. 2013. Fracture risk and height: an association partly accounted for by cortical porosity of relatively thinner cortices. J Bone Miner Res 28:2017–2026.

Bouvier M, Hylander WL. 1981. Effect of bone strain on cortical bone structure in macaques (Macaca mulatta). J Morphol 167:1–12.

Britz HM, Thomas CD, Clement JG, Cooper DM. 2009. The relation of femoral osteon geometry to age, sex, height and weight. Bone 45:77–83.

Burr DB, Milgrom C, Boyd RD, Higgins WL, Robin G, Radin EL. 1990. Experimental stress fractures of the tibia. Biological and mechanical aetiology in rabbits. J Bone Joint Surg Br 72:370–375.

Cho H, Stout SD, Bishop TA. 2006. Cortical bone remodeling rates in a sample of African American and European American descent groups from the American Midwest: comparisons of age and sex in ribs. Am J Phys Anthropol 130:214–226.

Courtland H-W, Nasser P, Goldstone AB, Spevak L, Boskey AL, Jepsen KJ. 2008. FTIRI microspectroscopy and micromechanical testing reveal intra-species variation in mouse bone mineral composition and matrix maturity. Calcif Tissue Int 83:342–353.

Currey JD. 1964. Some effects of ageing in human Haversian systems. J Anat 98:69–75.

Currey JD. 1979. Mechanical properties of bone tissues with greatly differing functions. J Biomech 12:313–319.
Currey JD, Alexander RM. 1985. The thickness of the walls of tubular bones. J Zool London 206:453–468.
Dellanini L, Hawkins D, Martin RB, Stover S. 2003. An investigation of the interactions between lower-limb bone morphology, limb inertial properties and limb dynamics. J Biomech 36:913–919.
Ekenman I, Halvorsen K, Westblad P, Fellander-Tsai L, Rolf C. 1998. Local bone deformation at two predominant sites for stress fractures of the tibia: an in vivo study. Foot Ankle Int 19:479–484.
Enlow DH. 1962. A study of the post-natal growth and remodeling of bone. Am J Anat 110:79–101.
Enlow DH. 1976. The remodeling of bone. Yearbook Phys Anthropol 20:19–34.
Epelboym Y, Gendron RN, Mayer J, Fusco J, Nasser P, Gross G, Ghillani R, Jepsen KJ. 2012. The inter-individual variation in femoral neck width is associated with the acquisition of predictable sets of morphological and tissue-quality traits and differential bone loss patterns. J Bone Miner Res 27:1501–1510.
Epker BN, Frost HM. 1966. Periosteal appositional bone growth from age two to age seventy in man. Anat Rec 154:573–578.
Ericksen MF. 1980. Patterns of microscopic bone remodeling in three aboriginal American populations. The Hague: Houton.
Eriksen EF, Steiniche T, Mosekilde L, Melsen F. 1989. Histomorphometric analysis of bone in metabolic bone disease. Endocrinol Metab Clin North Am 18:919–954.
Feik SA, Thomas CD, Clement JG. 1997. Age-related changes in cortical porosity of the midshaft of the human femur. J Anat 191 (Pt 3):407–416.
Frost HM. 1969. Tetracycline-based histological analysis of bone remodeling. Calcif Tissue Res 3:211–237.
Frost HM. 1987. Bone "mass" and the "mechanostat": a proposal. Anat Rec 219:1–9.
Goldman HM, Bromage TG, Boyde A, Thomas CD, Clement JG. 2003a. Intrapopulation variability in mineralization density at the human femoral mid-shaft. J Anat 203:243–255.
Goldman HM, Bromage TG, Thomas CD, Clement JG. 2003b. Preferred collagen fiber orientation in the human mid-shaft femur. Anat Rec 272A:434–445.
Goldman HM, McFarlin SC, Cooper DM, Thomas CD, Clement JG. 2009. Ontogenetic patterning of cortical bone microstructure and geometry at the human mid-shaft femur. Anat Rec (Hoboken) 292:48–64.
Goldman HM, Thomas CD, Clement JG, Bromage TG. 2005. Relationships among microstructural properties of bone at the human midshaft femur. J Anat 206:127–139.
Hamrick MW, Skedros JG, Pennington C, McNeil PL. 2006. Increased osteogenic response to exercise in metaphyseal versus diaphyseal cortical bone. J Musculoskelet Neuronal Interact 6: 258–263.
Hernandez CJ. 2008. How can bone turnover modify bone strength independent of bone mass? Bone 42:1014–1020.
Hildebrand M, Goslow G. 1998. Analysis of Vertebrate Structure. 5th ed. New York: Wiley.
Iwamoto J, Yeh JK, Aloia JF. 1999. Differential effect of treadmill exercise on three cancellous bone sites in the young growing rat. Bone 24:163–169.
Iwaniec UT, Crenshaw TD. 1998. Distribution of mineralization indices of modeling and remodeling over eight months in middiaphyseal cross sections of femurs from adult swine. Anat Rec 250: 136–145.
Jepsen KJ, Centi A, Duarte GF, Galloway K, Goldman H, Hampson N, Lappe JM, Cullen DM, Greeves J, Izard R, Nindl BC, Kraemer WJ, Negus CH, Evans RK. 2011. Biological constraints that limit compensation of a common skeletal trait variant lead to inequivalence of tibial function among healthy young adults. J Bone Miner Res 26:2872–2875.
Jepsen KJ, Evans R, Negus C, Gagnier JJ, Centi A, Erlich T, Hadid A, Yanovich R, Moran DS. 2013. Variation in tibial functionality and fracture susceptibility among healthy, young adults arises from the acquisition of biologically distinct sets of traits. J Bone Miner Res 28:1290–1300.
Jepsen KJ, Hu B, Tommasini SM, Courtland H-W, Price C, Terranova CJ, Nadeau JH. 2007. Genetic randomization reveals functional relationships among morphologic and tissue-quality traits that contribute to bone strength and fragility. Mamm Genome 18:492–507.
Jowsey J. 1966. Studies of Haversian systems in man and some animals. J Anat 100:857–864.
Kennedy OD, Herman BC, Laudier DM, Majeska RJ, Sun HB, Schaffler MB. 2012. Activation of resorption in fatigue-loaded bone involves both apoptosis and active pro-osteoclastogenic signaling by distinct osteocyte populations. Bone 50:1115–1122.
Kerley ER. 1965. The microscopic determination of age in human bone. Am J Phys Anthropol 23:149–163.
Lazenby R. 1986. Porosity-geometry interaction in the conservation of bone strength. J Biomech 19:257–258.
Lieberman DE, Pearson OM, Polk JD, Demes B, Crompton AW. 2003. Optimization of bone growth and remodeling in response to loading in tapered mammalian limbs. J Exp Biol 206:3125–3138.
Main RP. 2007. Ontogenetic relationships between in vivo strain environment, bone histomorphometry and growth in the goat radius. J Anat 210:272–293.
Martin RB, Pickett JC, Zinaich S. 1980. Studies of skeletal remodeling in aging men. Clin Orthop Relat Res:268–282.
Mason MW, Skedros JG, Bloebaum RD. 1995. Evidence of strain-mode-related cortical adaptation in the diaphysis of the horse radius. Bone 17:229–237.
McFarlin SC, Terranova CJ, Zihlman AL, Enlow DH, Bromage TG. 2008. Regional variability in secondary remodeling within long bone cortices of catarrhine primates: the influence of bone growth history. J Anat 213:308–324.
Meunier PJ, Boivin G. 1997. Bone mineral density reflects bone mass but also the degree of mineralization of bone: therapeutic implications. Bone 21:373–377.
Milgrom C, Giladi M, Simkin A, Rand N, Kedem R, Kashtan H, Stein M, Gomori M. 1989. The area moment of inertia of the tibia: a risk factor for stress fractures. J Biomech 22:1243–1248.
Mosekilde L. 2008. Primary hyperparathyroidism and the skeleton. Clin Endocrinol 69:1–19.
Pearson OM, Lieberman DE. 2004. The aging of Wolff's "law": ontogeny and responses to mechanical loading in cortical bone. Am J Phys Anthropol Suppl 39:63–99.
Pfeiffer S. 1980. Age changes in the external dimensions of adult bone. Am J Phys Anthropol 52:529–532.
Pfeiffer S, Lazenby R, Chiang J. 1995. Brief communication: cortical remodeling data are affected by sampling location. Am J Phys Anthropol 96:89–92.
Schlecht SH, Pinto DC, Agnew AM, Stout SD. 2012. Brief communication: the effects of disuse on the mechanical properties of bone: what unloading tells us about the adaptive nature of skeletal tissue. Am J Phys Anthropol 149:599–605.
Seibel MJ. 2002. Nutrition and molecular markers of bone remodelling. Curr Opin Clin Nutr Metab Care 5:525–531.
Skedros JG. 2012. Interpretting load history in limb-bone diaphyses: important considerations and their biomechanical foundations. In: Crowder C, Stout S, editors. Bone Histology: An Anthrological Perspective. Boca Raton: CRC Press. p 153–220.
Skedros JG, Hunt KJ, Bloebaum RD. 2004. Relationships of loading history and structural and material characteristics of bone: development of the mule deer calcaneus. J Morphol 259:281–307.
Skedros JG, Keenan KE, Williams TJ, Kiser CJ. 2013. Secondary osteon size and collagen/lamellar organization ("osteon morphotypes") are not coupled, but potentially adapt independently for local strain mode or magnitude. J Struct Biol 181:95–107.
Skedros JG, Mendenhall SD, Kiser CJ, Winet H. 2009. Interpreting cortical bone adaptation and load history by quantifying osteon morphotypes in circularly polarized light images. Bone 44:392–403.
Skedros JG, Su SC, Bloebaum RD. 1997. Biomechanical implications of mineral content and microstructural variations in cortical bone of horse, elk, and sheep calcanei. Anat Rec 249:297–316.
Stout SD, Crowder C. 2012. Bone remodeling, histomorphology, and histomorphometry. In: Crowder C, Stout S, editors. Bone Histology: An Anthropological Perspective. Bacon Raton, FL: CRC Press. p 1–22.

Stout SD, Lueck R. 1995. Bone remodeling rates and skeletal maturation in three archaeological skeletal populations. Am J Phys Anthropol 98:161–171.

Stout SD, Paine RR. 1994. Brief communication: bone remodeling rates: a test of an algorithm for estimating missing osteons. Am J Phys Anthropol 93:123–129.

Takahashi H, Epker B, Frost HM. 1965. Relation between age and size of osteons in man. Henry Ford Hosp Med Bull 13:25–31.

Thomas CD, Feik SA, Clement JG. 2005. Regional variation of intracortical porosity in the midshaft of the human femur: age and sex differences. J Anat 206:115–125.

Thomas CD, Feik SA, Clement JG. 2006. Increase in pore area, and not pore density, is the main determinant in the development of porosity in human cortical bone. J Anat 209:219–230.

Thompson DD. 1980. Age changes in bone mineralization, cortical thickness, and haversian canal area. Calcif Tissue Int 31:5–11.

Thompson DD, Gunness-Hey M. 1981. Bone mineral-osteon analysis of Yupik-Inupiaq skeletons. Am J Phys Anthropol 55:1–7.

Tommasini SM, Nasser P, Hu B, Jepsen KJ. 2008. Biological co-adaptation of morphological and composition traits contributes to mechanical functionality and skeletal fragility. J Bone Miner Res 23:236–246.

Tommasini SM, Nasser P, Jepsen KJ. 2007. Sexual dimorphism affects tibia size and shape but not tissue-level mechanical properties. Bone 40:498–505.

Tommasini SM, Nasser P, Schaffler MB, Jepsen KJ. 2005. Relationship between bone morphology and bone quality in male tibias: implications for stress fracture risk. J Bone Miner Res 20:1372–1380.

Turner CH. 1999. Site-specific skeletal effects of exercise: importance of interstitial fluid pressure. Bone 24:161–162.

Ural A, Vashishth D. 2006. Interactions between microstructural and geometrical adaptation in human cortical bone. J Orthop Res 24:1489–1498.

van Oers RF, Ruimerman R, Tanck E, Hilbers PA, Huiskes R. 2008a. A unified theory for osteonal and hemi-osteonal remodeling. Bone 42:250–259.

van Oers RF, Ruimerman R, van Rietbergen B, Hilbers PA, Huiskes R. 2008b. Relating osteon diameter to strain. Bone 43:476–482.

Verborgt O, Gibson GJ, Schaffler MB. 2000. Loss of osteocyte integrity in association with microdamage and bone remodeling after fatigue in vivo. J Bone Miner Res 15:60–67.

Walker RA, Lovejoy CO, Meindl RS. 1994. Histomorphological and geometric properties of human femoral cortex in individuals over 50: implications for histomorphological determination of age-at-death. Am J Hum Biol 6:659–667.

Zebaze RM, Ghasem-Zadeh A, Bohte A, Iuliano-Burns S, Mirams M, Price RI, Mackie EJ, Seeman E. 2010. Intracortical remodelling and porosity in the distal radius and post-mortem femurs of women: a cross-sectional study. Lancet 375:1729–1736.